LIQUIDICE

Deliverable D2.4 Glacier mass balance data set

eu-liquidice.eu

Funded by the European Union

Funded by the European Union. Views and opinions expressed are however those of the author(s) only and do not necessarily reflect those of the European Union or the European Climate, Infrastructure and Environment Executive Agency (CINEA). Neither the European Union nor the granting authority can be held responsible for them.

LIQUIDICE: LinkIng and QUantifying the Impacts of climate change on inlanD ICE, snow cover, and permafrost on water resources and society in vulnerable regions.

Funding programme: Horizon Europe
Project Start Date: 01.02.2025
Grant Agreement No.: 101184962
Duration: 48 months

Document information	
Work Package	2 - EO-based technologies for assessing the evolution of land ice and snow cover
Deliverable No.	2.4
Deliverable title	Glacier mass balance data set
Dissemination level	☒ PU - Public ☐ SEN - Sensitive
Lead Beneficiary	UNIVBRIS
Lead Author	Ritu Anilkumar
Contributors	UNIVBRIS
Contributing authors	Jonathan Bamber, Fabien Maussion
Due date	31.01.2026

Document history		
Version	1	
Version Date	30.01.2026	
Status	☒ Draft	28.01.2026
	☒WP leader approved	28.01.2026
	☒Coordinator approved	29.01.2026
	☒Executive Board / SST approved	30.01.2026

Table of Contents

Executive summary

This report pertains to the Deliverable D2.4: Glacier mass balance data set, as described in ANNEX 1, part A (p. 32) of the EC/REA Grant Agreement for project number 101184962, "LIQUIDICE". Work Package 2 of the LIQUIDICE project is led by NORCE with the support of CNR, IISC, IITB, GEUS, UNIVBRIS, SIOS-KC and IG PAS. Other beneficiaries are also asked to contribute to the deliverable by reaching out to key people and organisations in each of their own countries.

The accelerating loss of glacier mass is contributing to sea-level rise, disrupting ecosystems, reshaping hydrological regimes, increasing glacier-related hazards, undermining the resilience of dependent communities, and amplifying climate feedbacks through changes in albedo and freshwater fluxes. Quantifying annual glacier mass balance remains challenging because existing estimates rely on either sparse in situ and remote sensing observations or process-based models, each with inherent limitations. Observational approaches, while consistent at global scales, exhibit large regional variations. In contrast, modelling frameworks provide complete spatiotemporal fields but are typically deterministic, sensitive to calibration data, and constrained by assumptions that may overlook key energy balance drivers. Through our approach, we combined the strengths of models and various observational methods in a Bayesian neural network framework. Specifically, we used a Bayesian Neural Field architecture applied across all glacierized regions except those associated with the peripheral glaciers of Greenland and Antarctica. We pre-trained the Bayesian Neural Field model for each region using the Open Global Glacier Model (OGGM) fixed-geometry annual specific mass balance outputs from 1979–2019 as targets. The inputs were a suite of static glacier characteristics and dynamic near-surface meteorological predictors (air temperature, downwelling shortwave solar radiation, and total precipitation). Within this framework, we examined how various static and dynamic predictors, and their aggregations, influenced model performance in terms of accuracy and uncertainty. We demonstrate that predictors beyond temperature and precipitation are being used by our model to better represent the glacier mass balance processes. We evaluated the performance of the pre-trained model using a blocked testing strategy: (a) withholding 10% of glaciers to assess spatial performance, and (b) withholding 10% of years to assess temporal performance. Across regions, mean coefficients of determination were 0.72 (temporal) and 0.78 (spatial), with Root Mean Squared Error (RMSE) of 368.22 and 332.57 mm w.e. yr^{-1}, and median 95% interval widths of 781.88 and 925.57 mm w.e. yr^{-1}, respectively. This demonstrates the ability of the model to fill gaps for glaciers with missing or highly uncertain mass balance records as well as its capacity to reconstruct meaningful long-term time series that can be extended to assess glacier mass changes under future climate scenarios. Using this pre-trained framework, we estimate a global (excluding peripheral glaciers of Antarctica) total glacier mass change of –4242.2 Gt over 2000–2019. This provides a Bayesian prior that can be fine-tuned with multimodal observational datasets, including regionally aggregated altimetric and gravimetric records and temporally aggregated photogrammetric measurements.

1. Introduction

Glacier mass balance has historically been measured via the direct glaciological method, where a network of stakes and pits for measuring ablation and accumulation is used to measure point glacier mass balance. This is then extrapolated for the entire glacier. Subsequently, the geodetic glacier mass balance estimation technique emerged in the following forms: photogrammetric, interferometric, and LIDAR and RADAR altimetric surveys that generated a time series of elevations that could be differenced to generate changes in glacier thickness. This is subsequently converted into glacial volume changes and then glacial mass changes over a fixed period. The gravimetric method of glacier mass balance estimation uses satellite gravimetry (e.g., GRACE and GRACE-FO) to infer glacier mass changes from temporal variations in Earth's gravity field. After correcting for non-glacial signals (e.g., hydrology, glacial isostatic adjustment), the residual gravity anomalies provide coarse resolution estimates of glacier mass change. Recently, GlaMBIE, 2025 reported a consolidated account of glacier mass balance changes observed from 2000 to 2023 using the above-mentioned methods. They report −6542±387 Gt of cumulative mass loss over the period globally. All nineteen glacierised regions as defined in RGI depict a consistent glacier loss. Globally, a 5.4% cumulative loss was observed in 2023 when compared with the glacier mass in 2000. Regionally, Central Europe has seen the most significant relative mass loss at 38.7%. The Caucasus and Middle East saw a 35.3% loss, New Zealand saw 29.3%, Asia North saw 23.1%, Western Canada and USA saw 22.8%, South Asia East with the Eastern Himalayas saw 21.4%, and the low latitudes saw 20.2%. While these techniques are widely used in the measurement of mass balance, there are still several limiting factors that reflect as large uncertainties at the scale of a single glacier for any given year. Often, spatial and temporal aggregation of the measurements are performed to understand the underlying trends in a meaningful manner. For example, geodetic measurements from photogrammetry are estimated for every glacier as trends over 20 years (Hugonnet et al., 2021). Similarly, in GlaMBIE, 2025, annual measures of glacier mass change are derived at the regional scale.

Several models exist that estimate changes in glacier mass in response to meteorological factors. These are used in situations where measurements are not available, such as gaps in measurements spatially or temporally, or for understanding glacier mass change in the future. The models can be broadly categorised into full-physics models, temperature index models, and Machine Learning (ML) models. Typical full-physics models of glacier mass balance parameterise the primary energy balance components or use reanalysis estimates of the energy fluxes (shortwave, longwave, and turbulent) directly (e.g., Hock and Holmgren, 2005; Sauter et al., 2020). However, the performance of these models drops considerably with the unavailability of detailed glacier-level datasets, reduced quality of meteorological inputs as a result of extrapolating from the nearest weather stations, or the poor resolution of gridded meteorological data (Gabbi et al., 2014). Temperature index models simplify the ablation computation using temperature as a primary driving variable. These models use parameters such as melt factors and downscaling factors that are computed by calibrating to an existing observational dataset of glacier mass balance. Typical temperature index models are deterministic (e.g., Maussion et al., 2019; Zekollari et al., 2019), but there have been Bayesian formulations that permit uncertainty-aware modelling (e.g., Rounce et al., 2020). Known issues with temperature index models include oversensitivity to temperature and equifinality resulting from a larger number of parameters in the model and limited calibration datasets. ML models have been used to reduce the

oversensitivity to temperature by using various topographic and meteorological predictors (e.g., Bolibar et al., 2020; Anilkumar et al., 2023; Meer et al., 2025). However, they too have largely utilised only a subset of the data available due to the widely varying spatiotemporal scales at which the data is meaningful within the realms of uncertainty. Secondly, ML models, like most of the models described here, are primarily deterministic. Through this study, we attempt to develop a Bayesian Neural Network (BNN) that utilises a complete set of topographical and meteorological predictors to reconstruct glacier mass balance records that account for uncertainty in the prediction and allow for integration of datasets at varying spatio-temporal scales.

2. Data and Methods

We used the Bayesian Neural Field (BayesNF) framework to generate uncertainty-aware glacier mass balance predictions. BayesNF is a BNN architecture that was developed for spatiotemporal interpolation (e.g., Saad et al., 2024). It is a function-learning model that represents continuous fields and produces fully probabilistic outputs through variational inference or ensembles of Maximum Likelihood or Maximum A-Priori Estimates. It consists of explicitly creating covariates for the model through linear and Fourier combinations of inputs, a learnable scaling, learnable weight distributions, and a learnable combination of activation functions. Further, means to incorporate aleatoric uncertainty with the epistemic uncertainty are also included. We used the implementation available at: https://github.com/google/bayesnf. Please refer to the original publication for a complete description of the model architecture, inference method, and theoretical background.

The glacier mass balance estimates presented in this release were generated using a combination of meteorological forcing data, static glacier descriptors, and model-derived training targets. The following sections detail the experimental setup, the datasets used as inputs and targets to the model, and the evaluation strategy.

Data can be downloaded under the following link: https://zenodo.org/records/18417461

2.1. Experimental Setup

All machine learning models trained in a supervised regression framework use a set of input features (also called inputs, predictors, or covariates) that are combined non-linearly using some model parameters to generate an output. The outputs are compared with targets. The model parameters are modified such that the similarity between the outputs and targets is maximized. This process is called training the model. The similarity can be represented through various ways such as posterior probabilities (maximized represents maximum similarity) or loss/error functions (minimized represents maximum similarity). In order to test the performance of the models, we typically divide the entire available dataset into training and validation datasets. Most machine learning studies use random splits. However, we use blocked splitting with blocks in space and time to ensure independence of the performance evaluation as well as to ensure that the performance evaluation holds for gap filling in space or extrapolation in time. Specifically, we drop 10% of the glaciers and 10% of the years from the whole dataset and use the remainder as the training dataset. The dropped 10% of years (called LOYO) and glaciers (called LOGO) make up two validation sets which represent the ability of the trained model to accurately predict mass

balance estimates for unseen glaciers or years. The following years were left out from training: 1982, 1997, 1998, 2010, and 2019. Figure 1 represents the glaciers left out from the training. The intersection of glaciers and years left out were further removed from the validation datasets to perform independent testing. This dataset is called the LOGYO (leave 10% of the glaciers and years out) dataset.

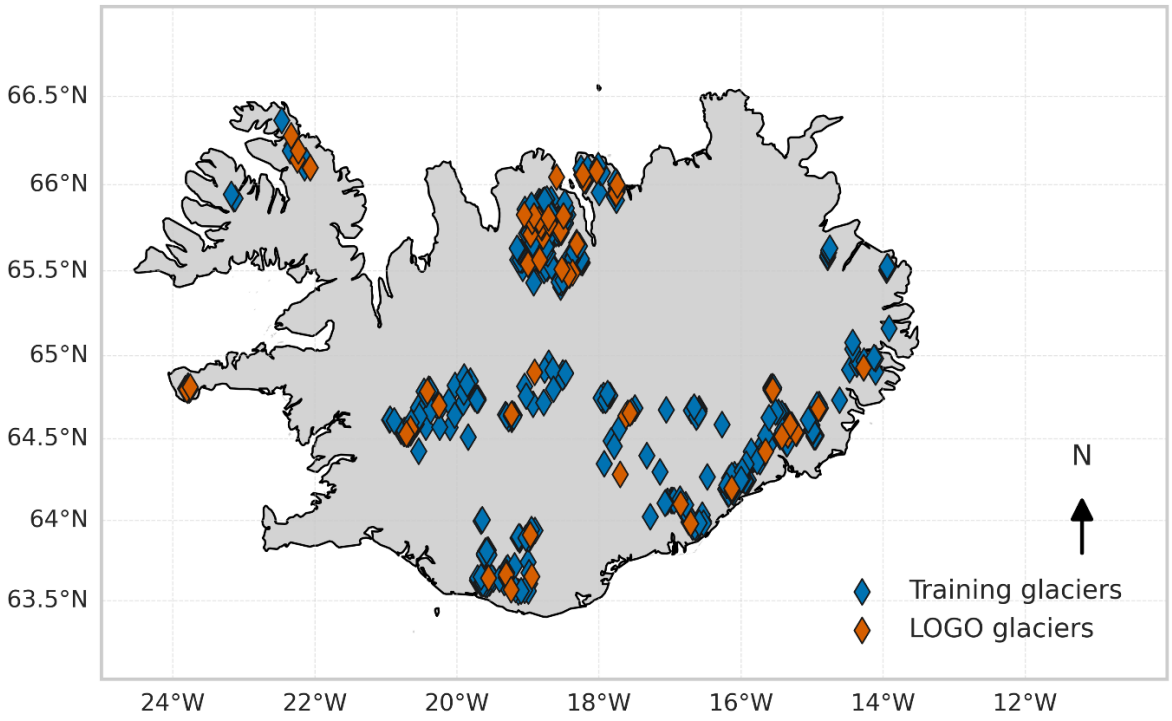

Figure 1: Spatial distribution of glaciers used for LOGO validation across Iceland. Blue symbols denote glaciers included in the training set, while orange symbols indicate glaciers withheld for validation under the LOGO scheme.

Several variants of the model were tested and the most optimal model was selected for each glacierized region defined as per RGI version 7. The search for the optimal model explored variations in meteorological datasets, network depth (number of hidden layers), network width (number of neurons per layer), input predictor combinations, and the application of input standardization. This systematic exploration was designed to assess model sensitivity to architectural complexity and feature representation. Each candidate model was trained for 10,000 epochs using region-specific training data. Model selection was based on performance evaluated on the validation dataset, ensuring that the chosen architectures were selected according to generalization behavior rather than training loss alone. Model performance was quantified using error metrics including coefficient of determination, RMSE, Median Absolute Error (MAE), and uncertainty metrics including the median interval width of 95% of ensemble members and coverage indicated by 95% of ensemble members. The best-performing architecture was identified separately for each glacierized region.

Following this hyperparameter tuning, the selected regional models were retrained for an extended period of 100,000 epochs. This extended training phase was intended to promote stable convergence and to allow robust estimation of predictive uncertainty. Retraining was conducted using the same regional data partitions.

2.2. Data Description

2.2.1. Inputs: Dynamic

We used dynamic meteorological predictors derived from global gridded reanalysis datasets. The variables evaluated included 2 m air temperature, total precipitation, and downwelling surface solar radiation. These variables were accessed from two reanalysis-based datasets and their performance was compared. The first dataset, ERA5-Land reanalysis, was accessed through Google Earth Engine, which aggregated the hourly ERA5-Land assets provided by the Copernicus Climate Data Store into monthly aggregates at 11 km spatial resolution. The second meteorological dataset used in this release is the Inter-Sectoral Impact Model Intercomparison Project (ISIMIP) WATCH Forcing Data methodology applied to ERA5 (W5E5) version 2.0 (doi: https://doi.org/10.48364/ISIMIP.342217; Lange et al., 2021). W5E5 combines the WATCH forcing applied on ERA5 data over land with unaltered ERA5 data over the ocean, providing a globally consistent meteorological dataset. W5E5 was tested as input to the BayesNF framework in addition to ERA5-Land because it was the forcing dataset for the Open Global Glacier Model (OGGM) simulations that produced the fixed-geometry specific mass balance targets used for training. The data of W5E5 are available at daily temporal resolution. Both datasets were considered for the period 1979 to 2019 and aggregated to various temporal scales. The temporal aggregations included (i) annual mean values together with minimum and maximum statistics, (ii) median values combined with standard deviations, (iii) seasonal means over summer and other months, and (iv) monthly aggregations. For precipitation, only the totals at the temporal aggregations were used, as it impacts the mass balance additively. All meteorological fields were spatially sampled over individual glacier centroids and temporally aligned with the corresponding mass balance observation periods prior to model input. We tested whether spatial aggregations over the glacier were feasible. However, due to very few glaciers exceeding the spatial resolution of the gridded data, we opted for spatial sampling for uniformity.

2.2.2. Input: Static

Static glacier predictors were derived from the RGI version 6, which provides global glacier outlines and associated geometric attributes. These predictors describe time-invariant glacier characteristics and include total glacier area, elevation statistics (minimum, median, and maximum elevation), slope, aspect, and glacier centroid coordinates (latitude and longitude). For each experiment, the static glacier predictors were combined with the aggregated dynamic meteorological variables to form the complete input feature set used by the BayesNF models. The data can be accessed from https://nsidc.org/data/nsidc-0770/versions/6.

2.2.3. (Pre)Training Targets

The supervised learning targets used in this study are derived from global simulations performed with the Open Global Glacier Model (OGGM). The OGGM simulations used in this release correspond to fixed-geometry annual specific mass balance outputs forced with the W5E5 version 2.0 meteorological dataset. The simulations cover the period 1979 to 2019. OGGM computes annual specific mass balance based on a temperature-index approach that is calibrated using available observational constraints from the per-glacier 20-year aggregation of Hugonnet et al. (2021). The OGGM outputs used in this study are publicly available and can be accessed through summary files at: https://cluster.klima.uni-bremen.de/~oggm/gdirs/oggm_v1.6/L3-L5_files/2023.3/. While this version consists of pretrained model outputs only, we plan that

these pretrained models will be fine-tuned on multimodal glacier mass balance observations at varying spatial and temporal scales in subsequent versions.

3. Results

3.1. Hyperparameter Tuning

In the initial attempts at hyperparameter tuning, we observed that annual inputs consistently did not train effectively. The trained model resulted in negative coefficients of determination for most regions; hence, they were not considered. Monthly and seasonal inputs performed better and were vigorously validated for all regions. For brevity, we demonstrate the hyperparameter tuning results over Iceland here and briefly describe the performance associated with all other regions.

Figure 2 represents the hyperparameter tuning for Iceland. This was used in selecting the optimal number of hidden layers and neurons and optimal predictors among seasonal and monthly predictors. While this figure represents the case for Iceland alone, a similar hyperparameter tuning was performed for all glacierized regions. Further, in situations where increasing the number of hidden neurons beyond 32 and the number of hidden layers beyond 2 resulted in improved performance, additional trials up to 512 hidden neurons and 4 layers were attempted. Across architectures, models with two hidden layers appear to achieve higher R^2 values in more instances than single-layer models under both LOYO and LOGO validation strategies. Under LOYO, R^2 improved markedly as the number of hidden neurons increased from 4 to 8, with only marginal gains beyond 16 neurons, indicating diminishing returns for larger networks. Seasonal predictors were preferred as indicated by LOYO validation, whereas monthly predictors were preferred for LOGO. This indicates that spatial gap filling was not impacted by temporal aggregation, but when extending the trained model to unseen years, seasonalities were important drivers. We emphasized LOYO compared to LOGO, as most glaciers have 20-year observations to constrain them and temporal extrapolation is more likely than spatial interpolation. Uncertainty estimates, quantified by the median 95% prediction interval width, generally decreased with increasing neuron count and layers, suggesting improved predictive sharpness for small-sized networks. However, gains in uncertainty reduction were modest beyond 16 neurons, and larger architectures did not consistently outperform smaller ones. We chose a network with one hidden layer and 16 hidden neurons with seasonal inputs as a favorable balance between predictive accuracy and uncertainty for the LOYO (preferred) and LOGO datasets for Iceland.

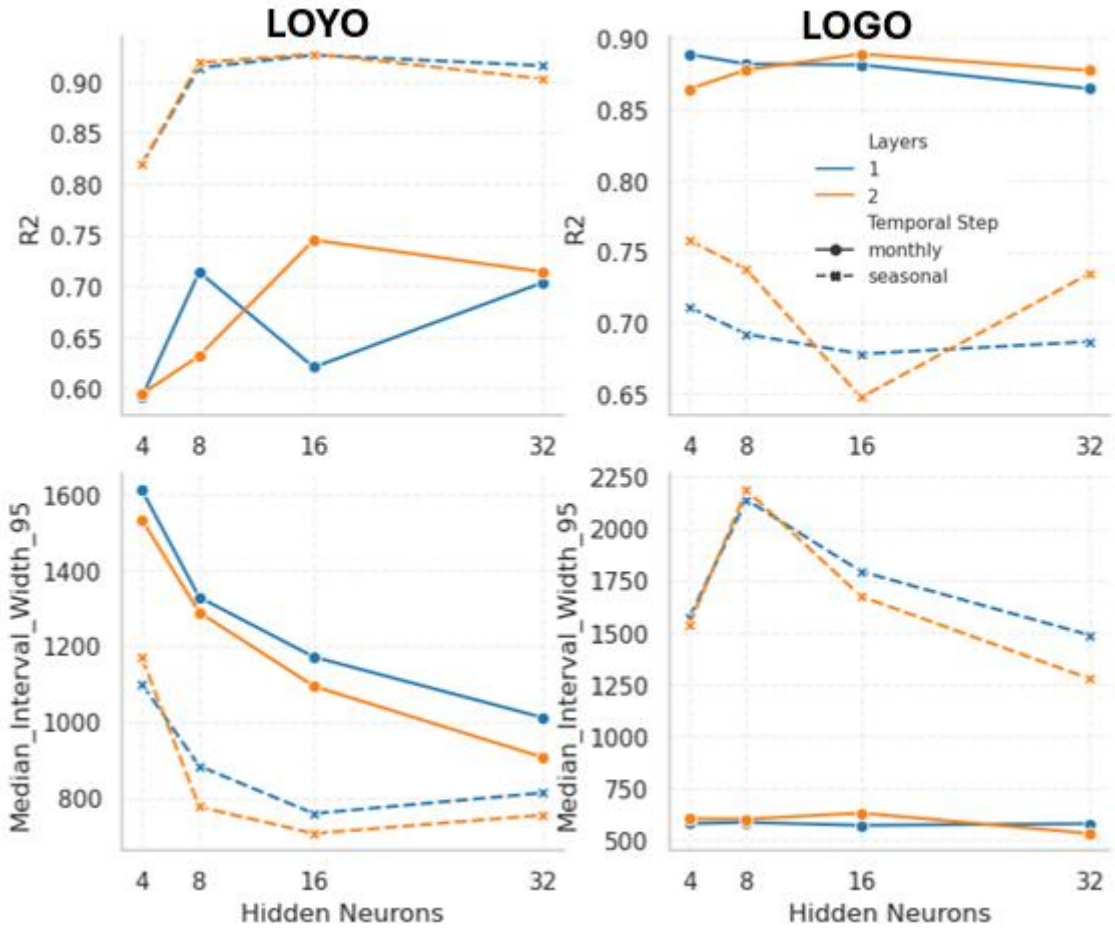

Figure 2: Hyperparameter sensitivity of model performance under LOYO (left column) and LOGO (right column) validation. Top panels show the coefficient of determination (R^2) and bottom panels show the median 95% prediction interval width as a function of the number

Similarly, hyperparameter tuning was performed for all RGI regions. Figure 3 summarizes model performance across the regions using the best-performing configuration (input temporal aggregate, number of hidden layers, number of hidden neurons) identified for each region under LOYO and LOGO validation. Substantial regional variability is evident in both validation strategies. Under LOGO, the coefficient of determination is generally high and stable across regions, with performance exceeding LOYO in 11 out of the 18 regions tested. Across regions, mean coefficients of determination were 0.72 (LOYO) and 0.78 (LOGO), with RMSE of 368.22 and 332.57 mm w.e. yr^{-1}, and median 95% interval widths of 781.88 and 925.57 mm w.e. yr^{-1}, respectively.

Overall, these results demonstrate that optimal model configurations and predictive performance are region dependent, and that performance under LOYO and LOGO validation can diverge substantially, emphasizing the importance of evaluating both temporal and spatial generalization when assessing glacier mass balance models and prioritizing the validation strategy relevant for the use case.

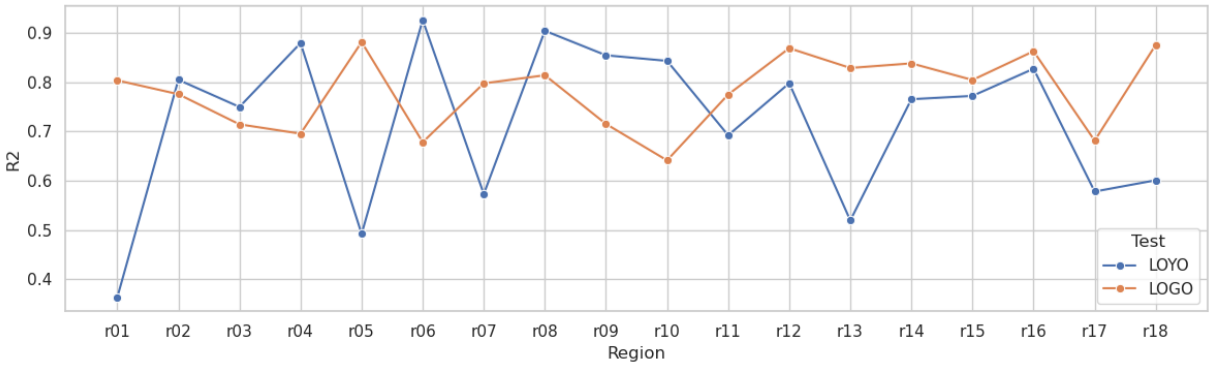

Figure 3: Coefficient of determination (R^2) for the best-performing models in each RGI region under LOYO (blue) and LOGO (orange) validation. Each point corresponds to the optimal hyperparameter configuration selected for a given region and validation strategy.

3.2. Validation and Testing Performance of Best Model

Figure 4 presents model performance under LOYO and LOGO validation, including predicted versus observed mass balance scatter plots of the LOYO validation dataset and a representative time-series example from the LOGO dataset. Under LOYO validation, predictions show strong agreement with observations, with points tightly clustered around the 1:1 line. The model achieves a high coefficient of determination (R^2 = 0.93), along with relatively low error metrics (RMSE = 285.9 mm w.e. yr^{-1}; MedAE = 224.0 mm w.e. yr^{-1}), indicating its ability to reproduce interannual mass balance variability within individual glaciers. Model performance is reduced under LOGO validation, where entire glaciers are excluded from training. The predicted versus observed relationship exhibits increased scatter, reflected in a lower R^2 value of 0.68 and higher error metrics (RMSE = 398.0 mm w.e. yr^{-1}; MedAE = 238.9 mm w.e. yr^{-1}). These results indicate decreased predictive accuracy when generalizing across glaciers compared to temporal extrapolation within the same glacier.

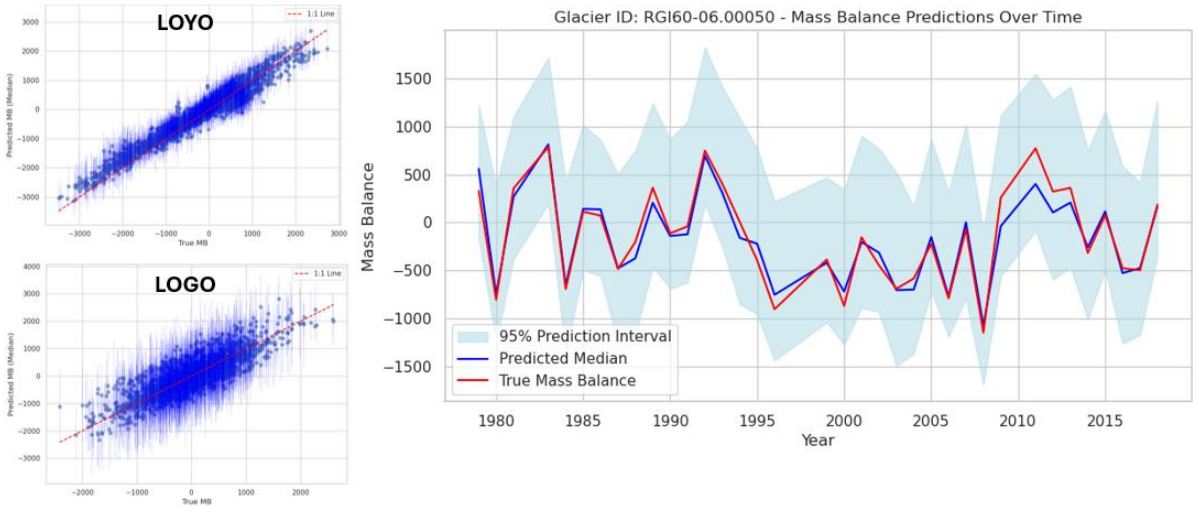

Figure 4: Model performance under LOYO and LOGO validation. Scatter plots show predicted versus observed annual glacier-wide mass balance for the LOYO (top left) and LOGO (bottom left) validation datasets, with the red dashed line indicating the 1:1 relationship

The time-series example for a glacier in the LOGO validation set (RGI60-06.00050) illustrates the model's behavior under LOGO validation. The predicted median mass balance follows the overall temporal evolution of the observed series, capturing the timing and sign of major anomalies. The

observed mass balance generally falls within the predicted 95% prediction interval. However, note that the uncertainty interval is quite large, and so this can be expected.

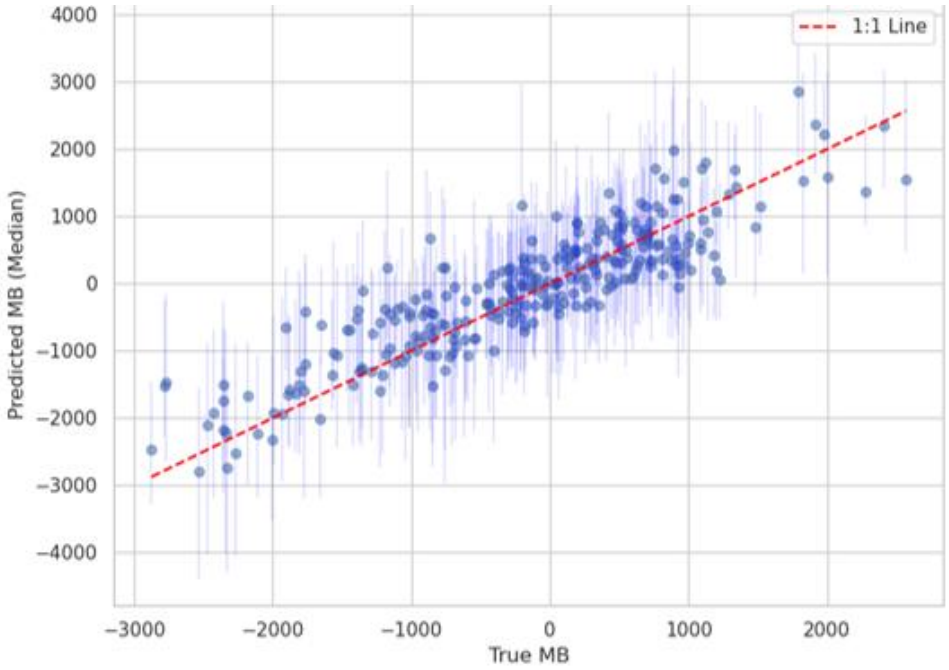

Figure 5: Predicted versus observed annual glacier-wide mass balance under LOGYO validation. Each point represents a withheld glacier–year pair, with vertical bars indicating the 95% prediction interval. The red dashed line denotes the 1:1 relationship

Uncertainty characteristics differ substantially between validation strategies. Prediction intervals are markedly narrower under LOYO, with a median interval width of 759.0 mm w.e. yr^{-1}, compared to 1793.4 mm w.e. yr^{-1} under LOGO. Correspondingly, empirical coverage is higher for LOGO (93.6%) than for LOYO (80.5%). These results indicate sharper but less conservative uncertainty estimates for temporal holdout, and broader, more conservative uncertainty estimates when predicting mass balance for previously unseen glaciers.

Figure 5 shows the predicted versus observed mass balance relationship under LOGYO validation. The scatter plot indicates that the trained models perform well while generalizing across both unseen glaciers and unseen years simultaneously. The coefficient of determination is $R^2 = 0.77$. Error metrics are correspondingly higher, with RMSE = 489.7 mm w.e. yr^{-1} and MedAE = 313.0 mm w.e. yr^{-1}, indicating degraded performance relative to both single-dimension holdout schemes.

Uncertainty estimates under LOGYO are also broader, with a median prediction interval width of 1904.0 mm w.e. yr^{-1}, slightly exceeding that of LOGO and substantially larger than under LOYO. Empirical coverage reaches 91.2%, suggesting that prediction intervals remain largely well calibrated despite the increased difficulty of the task. This is expected, as there are no representative data available in the training and the model does not produce overconfident uncertainty bounds.

3.3. The Glacier Mass Balance Product

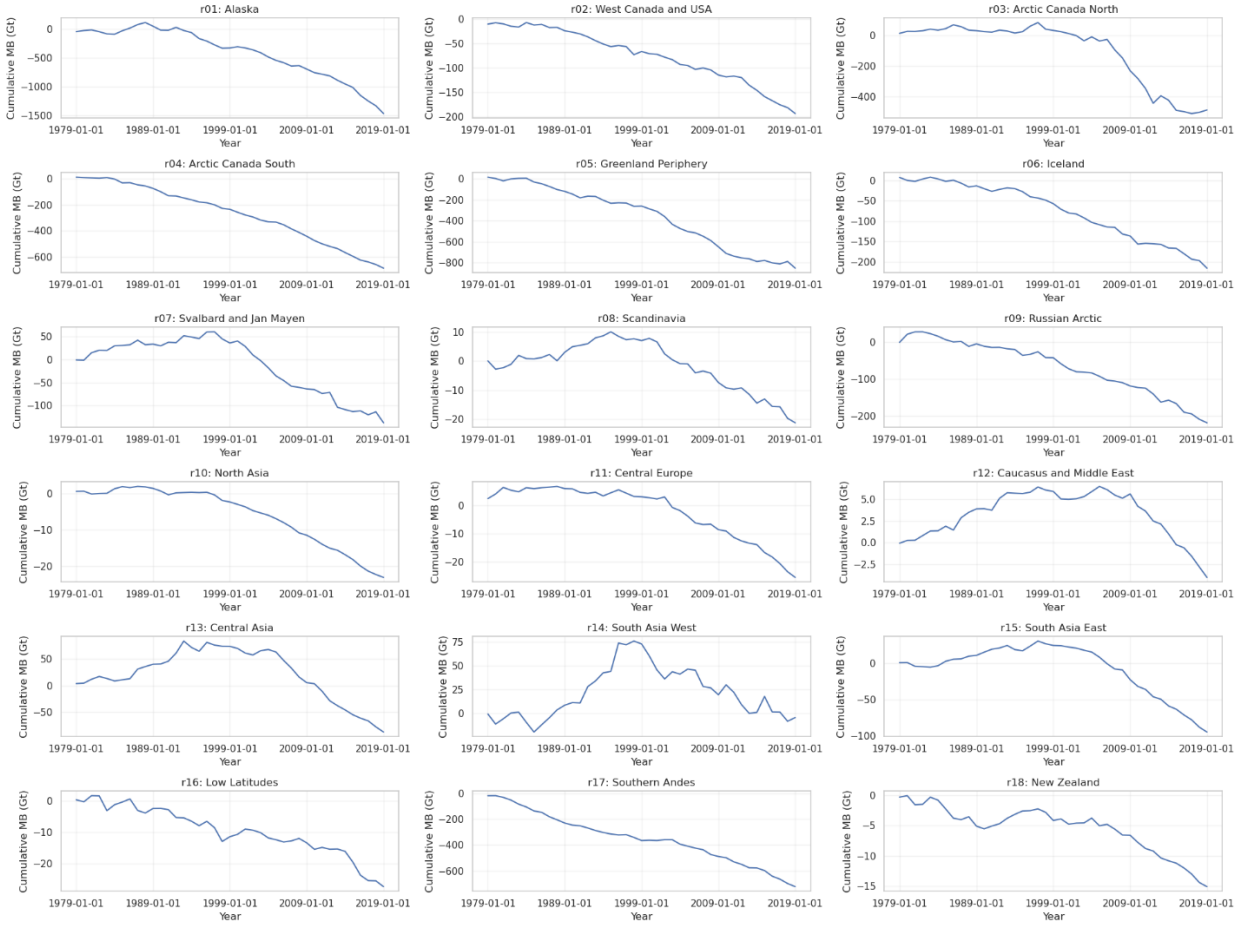

Figure 6: Cumulative glacier mass balance by RGI region (r01–r18) from 1979 to 2019. Values

This dataset provides annual glacier mass balance estimates derived using an uncertainty-aware machine learning framework based on Bayesian Neural Fields. The dataset covers all glacierized regions defined in RGIv7 except Regions 19 and 20 (19: Sub-Antarctic and Antarctic Islands; 20: Antarctic Mainland). Temporal coverage spans 1979–2019. This dataset is intended as a global, consistent Bayesian prior for glacier mass balance. This is a preliminary release of pretrained outputs; dataset structure is subject to significant change after fine-tuning on observations. The data repository contains annual glacier mass balance estimates for all the glaciers in the study region. It can be found at the following doi: 10.5281/zenodo.18417461

Figure 6 shows cumulative glacier mass change derived from our method for all RGI regions considered in this study. All regions exhibit a long-term decline in cumulative mass balance, with the magnitude and temporal evolution varying substantially by region. Summing over all regions yields a global cumulative glacier mass change of −4080.2 Gt over 2000–2019. This estimate is in close agreement with the GLAMBIE combined product (corrected to exclude Antarctica, over which our simulations have not been run yet), which reports a corresponding global loss of −4242.2 Gt over the same period. The difference between the two estimates (162 Gt, or ~3.8%) is small relative to the total signal and within the realm of uncertainties. Regionally, Region 1 (Alaska) has lost the most glacier mass, followed by the Greenland periphery and Arctic Canada North.

4. Future Directions

The glacier mass balance estimates presented here represent a preliminary product derived from a Bayesian Neural Field framework pretrained on model-derived targets. While the results demonstrate strong spatial and temporal generalization performance and close agreement with independent global assessments, several limitations remain that constrain the current interpretation and highlight priorities for future versions.

The current dataset spans 1979–2019 and excludes RGI Regions 19 (Sub-Antarctic and Antarctic Islands) and the ice sheet mass balance. We hope to extend our results to cover the ice sheet mass balance and Region 19 glaciers for the years 1950–present in future releases. It is important to note that we have considered only elevation differences at the moment and ignored changes in glacier area and density. This assumption neglects dynamic glacier retreat and hypsometric evolution, which may influence mass balance sensitivity to climate forcing over multidecadal periods. Incorporating time-varying glacier geometry from inventories or area–volume scaling approaches would allow the model to account explicitly for geometric feedbacks and is a natural extension of the present framework.

In its current form, the Bayesian Neural Field is trained using fixed-geometry annual specific mass balance outputs from OGGM forced by W5E5 meteorological data. As a result, the present estimates should be interpreted as a probabilistic reconstruction of OGGM-consistent mass balance rather than an observation-driven product. Although OGGM is calibrated using multidecadal geodetic constraints, any structural biases or simplifications in the temperature-index formulation may be reflected in the machine-learning model. At the moment, this is meant to be a prior on the parameter distribution, i.e., a probabilistic prior for glacier mass balance suitable for integration into machine learning modelling of glacier mass balance. It is not intended as a definitive observational product. Future releases will focus on fine-tuning the pretrained models using multimodal observational datasets, including regional altimetric and gravimetric mass balance products and temporally aggregated photogrammetric measurements.

References

1. Anilkumar, R. et al. (2023). “Modelling point mass balance for the glaciers of the Central European Alps using machine learning techniques”. In: The Cryosphere 17.7, pp. 2811–2828.
2. Bolibar, J. et al. (2020). “Deep learning applied to glacier evolution modelling”. In: The Cryosphere 14.2, pp. 565–584.
3. Gabbi, J. et al. (2014). “A comparison of empirical and physically based glacier surface melt models for long-term simulations of glacier response”. In: Journal of Glaciology 60.224, pp. 1140–1154. DOI: 10.3189/2014JoG14J011.
4. GlaMBIE (2025). “Community estimate of global glacier mass changes from 2000 to 2023”. In: Nature 639.8054, pp. 382–388. ISSN: 1476-4687. DOI: 10.1038/s41586-024-08545-z. URL: https://doi.org/10.1038/s41586-024-08545-z.
5. Hock, R. and B. Holmgren (2005). “A distributed surface energy-balance model for complex topography and its application to Storglaciären, Sweden”. In: Journal of Glaciology 51.172, pp. 25–36. DOI: 10.3189/172756505781829566.

6. Hugonnet, R. et al. (2021). "Accelerated global glacier mass loss in the early twenty-first century". In: Nature 592.7856, pp. 726–731. DOI: https://doi.org/10.1038/s41586-021-03436-z.
7. Lange, S. et al. (2021). WFDE5 over land merged with ERA5 over the ocean (W5E5 v2.0).
8. Maussion, F. et al. (2019). "The open global glacier model (OGGM) v1.1". In: Geoscientific Model Development 12.3, pp. 909–931.
9. Meer, M. van der et al. (2025). "A minimal machine-learning glacier mass balance model". In: The Cryosphere 19.2, pp. 805–826.
10. Rounce, D. R., R. Hock, and D. E. Shean (2020). "Glacier mass change in High Mountain Asia through 2100 using the open-source python glacier evolution model (PyGEM)". In: Frontiers in Earth Science 7, p. 331.
11. Saad, F. et al. (2024). "Scalable spatiotemporal prediction with Bayesian neural fields". In: Nature Communications 15.1, p. 7942.
12. Sauter, T., A. Arndt, and C. Schneider (2020). "COSIPY v1.3 – an open-source coupled snowpack and ice surface energy and mass balance model". In: Geoscientific Model Development 13.11, pp. 5645–5662. DOI: 10.5194/gmd-13-5645-2020. URL: https://gmd.copernicus.org/articles/13/5645/2020/
13. Zekollari, H., M. Huss, and D. Farinotti (2019). "Modelling the future evolution of glaciers in the European Alps under the EURO-CORDEX RCM ensemble". In: The Cryosphere 13.4, pp. 1125–1146. DOI: 10.5194/tc-13-1125-2019. URL: https://tc.copernicus.org/articles/13/1125/2019/.

***